

---

# Repeating and Non-repeating Fast Radio Bursts from Binary Neutron Star Mergers

Shotaro YAMASAKI<sup>1</sup>, Tomonori TOTANI,<sup>1,2</sup> and Kenta KIUCHI<sup>3</sup>

<sup>1</sup>Department of Astronomy, School of Science, The University of Tokyo, 7-3-1 Hongo, Bunkyo-ku, Tokyo 113-0033, Japan

<sup>2</sup>Research Center for the Early Universe, School of Science, The University of Tokyo, 7-3-1 Hongo, Bunkyo-ku, Tokyo 113-0033, Japan

<sup>3</sup>Center for Gravitational Physics, Yukawa Institute for Theoretical Physics, Kyoto University, Kyoto 606-8502, Japan

\*E-mail: yamasaki@astron.s.u-tokyo.ac.jp

Received ; Accepted

## Abstract

Most of fast radio bursts (FRB) do not show evidence for repetition, and such non-repeating FRBs may be produced at the time of a merger of binary neutron stars (BNS), provided that the BNS merger rate is close to the high end of the currently possible range. However, the merger environment is polluted by dynamical ejecta, which may prohibit the radio signal to propagate. We examine this by using a general-relativistic simulation of a BNS merger, and show that the ejecta appears about 1 ms after the rotation speed of the merged star becomes the maximum. Therefore there is a time window in which an FRB signal can reach outside, and the short duration of non-repeating FRBs can be explained by screening after ejecta formation. A fraction of BNS mergers may leave a rapidly rotating and stable neutron star, and such objects may be the origin of repeating FRBs like FRB 121102. We show that a merger remnant would appear as a repeating FRB in a time scale of  $\sim 1$ –10 yrs, and expected properties are consistent with the observations of FRB 121102. We construct an FRB rate evolution model including these two populations of repeating and non-repeating FRBs from BNS mergers, and show that the detection rate of repeating FRBs relative to non-repeating ones rapidly increases with improving search sensitivity. This may explain that the only repeating FRB 121102 was discovered by the most sensitive FRB search with Arecibo. Several predictions are made, including appearance of a repeating FRB 1–10 years after a BNS merger that is localized by gravitational wave and subsequent electromagnetic radiation.

**Key words:** stars: neutron — stars: binaries: general — gravitational waves — radio continuum: general

---

## 1 Introduction

The enigmatic millisecond-duration radio transients, the so-called fast radio bursts (FRBs) were first discovered by Lorimer et al. (2007), then confirmed with additional four bursts by Thornton et al. (2013), and now it is an intensive field of research in astronomy. About 20 FRBs have been reported to date (Petroff et al. 2016), but their origin and physical mechanism still remain mysterious. Their dispersion measures (DMs)

$DM \equiv \int n_e dl = 300$ –1500 pc cm<sup>-3</sup> (Petroff et al. 2016) are much larger than those expected for objects in the Milky Way, and a cosmological distance scale of  $z \sim 1$  is inferred if the dominant contribution to DMs is from electrons in ionized intergalactic medium (IGM). Counterparts in other wavelengths or host galaxies have not yet been detected in most cases. Keane et al. (2016) reported a radio afterglow of FRB 150418 and identification of an elliptical host galaxy at  $z = 0.492$ , but there is

a claim that the radio afterglow may be an AGN activity that is not related to the FRB (Williams & Berger 2016).

The majority of FRBs do not show evidence for repetition, in spite of the fact that some of them have been intensively monitored to search possible repeating bursts (Lorimer et al. 2007; Petroff et al. 2015). The only exception is FRB 121102, which is the only FRB discovered by the Arecibo observatory (Spitler et al. 2014) and later found to repeat (Spitler et al. 2016; Scholz et al. 2016). The repetition allowed sub-arcsecond localization and the first unambiguous identification of the host galaxy (Chatterjee et al. 2017; Marcote et al. 2017; Tendulkar et al. 2017). FRB 121102 was discovered by a high-sensitivity search of Arecibo, and its burst flux ( $\sim 0.02\text{--}0.3$  Jy) is smaller than that of other FRBs ( $\sim 0.2\text{--}2$  Jy) mostly detected by the Parkes observatory (Spitler et al. 2016). If we take into account distance ( $z = 0.193$  for FRB 121102 and the DM-inferred redshifts of  $z = 0.5\text{--}1.0$  for other FRBs), the absolute luminosity of FRB 121102 is two orders of magnitude smaller than other FRBs. This implies a possibility that FRB 121102 belongs to a different population from other FRBs.

There is a variety of progenitor models proposed for FRBs; some of them are related to repeatable populations, while others to catastrophic events. The former includes giant flares from soft gamma-ray repeaters (SGRs; Popov & Postnov 2010; Thornton et al. 2013; Lyubarsky 2014; Kulkarni et al. 2014), giant radio pulses from pulsars (Connor et al. 2016; Cordes & Wasserman 2016), repeating FRBs from a young neutron star (Kashiyama & Murase 2017; Metzger et al. 2017; Beloborodov 2017), collisions of asteroids with a neutron star (Geng & Huang 2015; Dai et al. 2016), and pulsars interacting with plasma stream (Zhang 2017). The latter includes binary neutron star (or black hole) mergers (Totani 2013; Mingarelli et al. 2015), binary white dwarf mergers (Kashiyama et al. 2013), and collapsing supermassive neutron stars (Falcke & Rezzolla 2014).

In this paper we consider mergers of binary neutron stars (BNS, i.e., a binary of two neutron stars) as a possible source of FRBs. Apparently non-repeating FRBs can be explained by radio emission at the time of merger. The exceptionally intense FRB 150807 shows a small amount of rotation measure (RM) implying negligible magnetization in the circum-burst plasma (Ravi et al. 2016), which may favor the clean environment expected around BNS mergers. There is still a large uncertainties in both FRB and BNS merger rates, but the FRB event rate is close to the high end of the plausible range of BNS merger rate,  $1 \times 10^4 \text{ Gpc}^{-3} \text{ yr}^{-1}$  (Abadie et al. 2010). The latest upper bound on the BNS merger rate by LIGO (Abbot et al. 2016) is also close to this:  $1.26 \times 10^4 \text{ Gpc}^{-3} \text{ yr}^{-1}$  (90% C.L.), indicating that a BNS merger should be detected soon if non-repeating FRBs are produced by BNS mergers. The observed FRB flux can be explained by magnetic braking luminosity and a radio

conversion efficiency similar to pulsars (Totani 2013). Wang et al. (2016) investigated radio emission based on the unipolar inductor model (Piro 2012; Lai 2012, see also Hansen & Lyutikov 2001).

A theoretical concern of the BNS merger scenario is, however, that the environment around the merger would be polluted by matter dynamically expelled during the merger process, which may prohibit the radio signal to be transmitted. The first aim of this work is to investigate this issue by using a numerical-relativity simulation of a BNS merger. We will compare the rise of rotation power that may produce an FRB and the timing of dynamical matter ejection, and examine whether there is a time window in which an FRB is produced and transmitted to an observer.

It is obvious that a radio burst at the time of a BNS merger cannot explain the repeating FRB 121102. A young neutron star possibly with strong magnetic field (i.e., a magnetar) is then popularly discussed as the source of FRB 121102, which is surrounded by a pulsar wind nebula (PWN) that is responsible for the observed persistent radio emission. Therefore a core-collapse supernova, especially in the class of superluminous supernovae (SLSNe), is discussed as the progenitor of FRB 121102, because formation of a rapidly rotating magnetar is one of the possible explanations for the extreme SLSN luminosity, and because of the host galaxy properties (dwarf and low metallicity) (Kashiyama & Murase 2017; Metzger et al. 2017).

However, a fraction of BNS mergers may leave a massive neutron star which is indefinitely stable or temporarily stable by a rotational support (e.g., Gao et al. 2013; Metzger & Piro 2014; Piro et al. 2017). The fraction strongly depends on the equation of state (EOS) for nuclear matter, which may be either negligible or the majority. The later requires that EOS is stiff enough to support a spherical neutron star with the maximum mass of  $\gtrsim 2.7M_{\odot}$ . Such remnant neutron stars should be rapidly spinning by the large angular momentum of the original binary, and their magnetic field can be amplified by the merger process (e.g., Kiuchi et al. 2014), possibly to the magnetar level. The ejecta mass from a BNS merger is much smaller than SLSNe, making the transmission of radio signal easier. The estimated event rate of BNS mergers is higher than that of SLSNe by 1–2 orders of magnitude (Abadie et al. 2010; Quimby et al. 2013), and hence the production rate of rapidly rotating neutron stars by BNS mergers may be higher than that by SLSNe.

The second aim of this work is to examine merger-remnant neutron stars as the origin of repeating FRBs like FRB 121102. We make order-of-magnitude estimates of various physical quantities and compare with the observational constraints for FRB 121102. We then propose a unified scenario for repeating and non-repeating FRBs from BNS mergers. Non-repeating and bright FRBs are produced as a single catastrophic event at the time of merger, while repeating and faint FRBs are produced by

young and rapidly rotating neutron stars left after BNS mergers. We then present an FRB rate evolution model including these two populations, and examine the relative detection rate as a function of search sensitivity. This may give a hint to explain the fact that the only repeating FRB was detected as the faintest FRB.

The outline of this paper is as follows. In section 2, we describe the details of the BNS simulation used in this work. We then examine ejecta formation by the merger and discuss the possibility of producing a non-repeating FRB in section 3. The merger-remnant neutron star scenario for repeating FRBs is compared with the available observational constraints in section 4, and the FRB rate evolution model is presented in section 5. Conclusions will be given with some discussions in section 6. The adopted cosmological parameters for a flat universe are  $H_0 = 67.8 \text{ km s}^{-1} \text{ Mpc}^{-1}$ ,  $\Omega_M = 0.308$ , and  $\Omega_\Lambda = 0.692$  (Planck Collaboration et al. 2016).

## 2 BNS Merger Simulation

Methods of the BNS merger simulation used in this work are presented in Kiuchi et al. (2014). The simulation employs the moving puncture gauge, and the spatial coordinates (denoted by  $xyz$ ) are defined so that they asymptotically become the Cartesian coordinate system towards a point at infinity from the center. The simulation is performed in a cubic box and the centers of two neutron stars are located in the  $z = 0$  plane. A reflection symmetry with respect to the  $z = 0$  plane is assumed. A fixed mesh-refinement algorithm with seven levels is adopted for the spatial coordinates to resolve the wide dynamic range of a BNS merger. The outermost (i.e., the first level) box has  $469 \times 469 \times 235$  grids in  $x$ - $y$ - $z$ , with a grid size of  $\sim 9.6$  km. (The number of  $z$ -direction grids is only for the upper half of the cube.) In the second level, the box of half size (i.e., 1/8 in volume) with the same box center is simulated with a two times finer grid size, while the grid number is the same. This is repeated in the same way to the seventh level where the mesh size is  $1/2^6$  of the first level ( $\sim 150$  m).

We employ the H4 EOS of Glendenning & Moszkowski (1991), with which the maximum mass of neutron stars is  $2.03 M_\odot$ . Two neutron stars have the same ADM mass of  $1.35 M_\odot$  when they are isolated. This simulation does not include magnetic fields; there are no known BNS simulations in which dynamical ejecta mass is significantly changed by the effects of magnetic fields. The simulation starts with an orbital angular velocity  $\Omega_{\text{orb}} \sim 1.7 \times 10^3 \text{ s}^{-1}$  and a binary separation of  $\sim 50$  km, and the merger occurs after several in-spiral orbits. The simulation finishes at 15 ms after the merger, and at that time the merged hypermassive neutron star (HMNS) is still rotationally supported against a gravitational collapse.

Our purpose is to investigate the time evolutionary proper-

ties of matter ejected to outer regions, and we do not have to examine quantitatively the general relativistic effects that are important around the merger center. Therefore in this work we present physical quantities assuming that the simulation grids are on the classical Cartesian coordinate system throughout the box, and the simulation time grids are on the classical time coordinate.

For computational reasons, numerical simulations of a BNS merger usually set an artificial atmosphere around stars, and in our simulation the density of atmosphere is  $10^3 \text{ g cm}^{-3}$  within  $r \leq 70$  km and it decreases as  $\propto r^{-3}$  in outer regions, where  $r$  is the radius from the simulation center. The central density of the atmosphere is  $10^{12}$  times smaller than the nuclear matter density found inside the neutron stars. Furthermore, the minimum density that the simulation can reliably resolve is  $\sim 10^8 \text{ g cm}^{-3}$ . Therefore we consider only matter whose density is higher than the threshold value,  $\rho_{\text{th}} = 10^8 \text{ g cm}^{-3}$ , when calculating the rest-mass column density of ejecta. Even if calculated column density allows transmission of FRB signals, we cannot exclude a possibility that lower density material than  $\rho_{\text{th}}$  absorbs FRB signals. However, our results shown below indicate that the matter density rapidly drops at a certain radius from the HMNS, and material of  $\rho < \rho_{\text{th}}$  would unlikely affect our main conclusions.

## 3 Environment around the merger and FRB possibility

### 3.1 Orbital evolution and neutron star spin-up

Figure 1 presents time snapshots of density contours and velocity fields of the simulation, spanning from 0.71 ms before to 4.26 ms after the merger, where the merger time  $t_{\text{merge}}$  is defined as the time when the density peaks of the two neutron stars merge into one.

FRBs are expected to be generated by rotation, either the orbital motion of the two neutron stars or spins of individual neutron stars. The rotation angular velocity of the orbital motion ( $\Omega_{\text{orb}}$ ) and that of the individual neutron star spin ( $\Omega_{\text{spin}}$ ) are shown as a function of time in figure 2. For this calculation, we first calculate the angular velocity at each grid from the rotation-direction component of fluid velocity, as

$$\Omega(\mathbf{r}) = \frac{1}{|\mathbf{r}_{xy}|} \mathbf{v} \cdot \left( \frac{\mathbf{n}_z \times \mathbf{r}}{|\mathbf{n}_z \times \mathbf{r}|} \right), \quad (1)$$

where  $\mathbf{r}$  is the position vector measured from the rotation center on the  $z = 0$  plane,  $\mathbf{v}$  the three velocity of fluid,  $\mathbf{n}_z$  the unit spatial vector to the  $z$  direction, and  $\mathbf{r}_{xy}$  the projection of  $\mathbf{r}$  onto the  $xy$  plane. Then the average rotation velocity is calculated as the mass-weighted mean:

$$\Omega_{\text{av}} = \frac{\int \Omega(\mathbf{r}) \rho(\mathbf{r}) d\mathbf{r}}{\int \rho(\mathbf{r}) d\mathbf{r}}, \quad (2)$$

where  $\rho$  is the rest-mass density. The orbital rotation veloc-

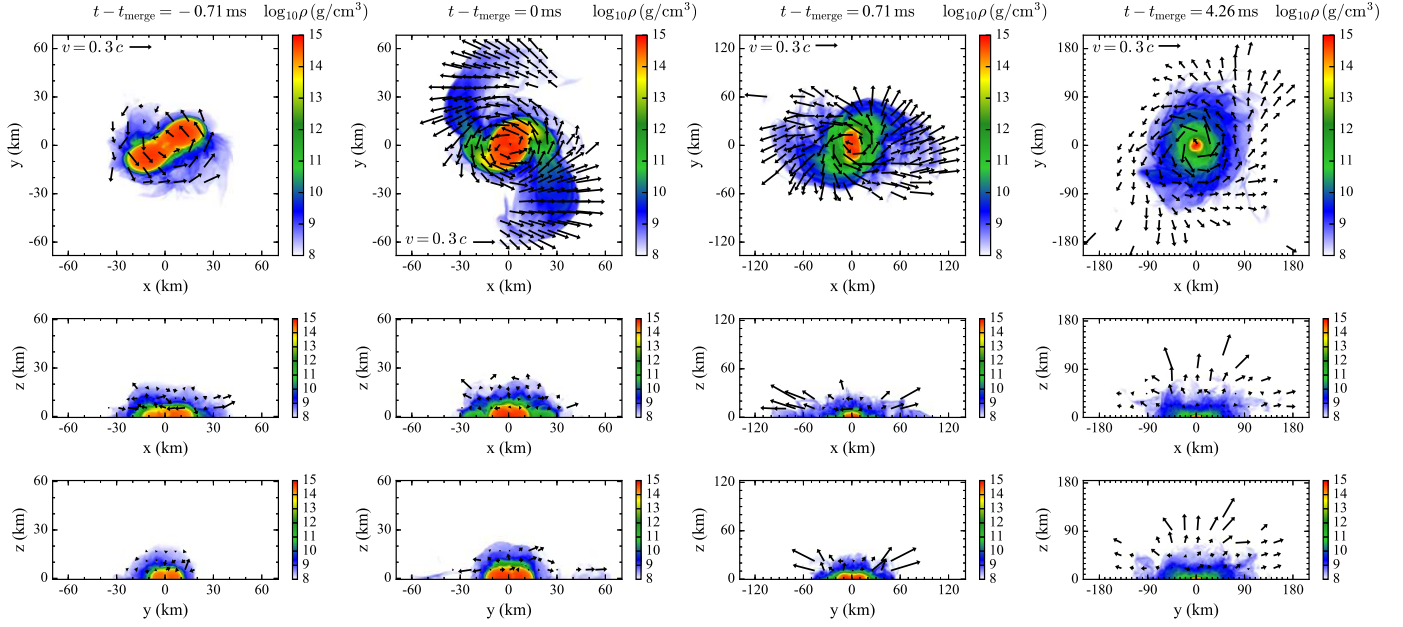


**Fig. 1.** Time snapshots of density contours for the binary neutron star merger simulation used in this work, in the  $xyz$  coordinates which are approximately the classical Cartesian coordinates. The velocity fields are also shown by black vectors.

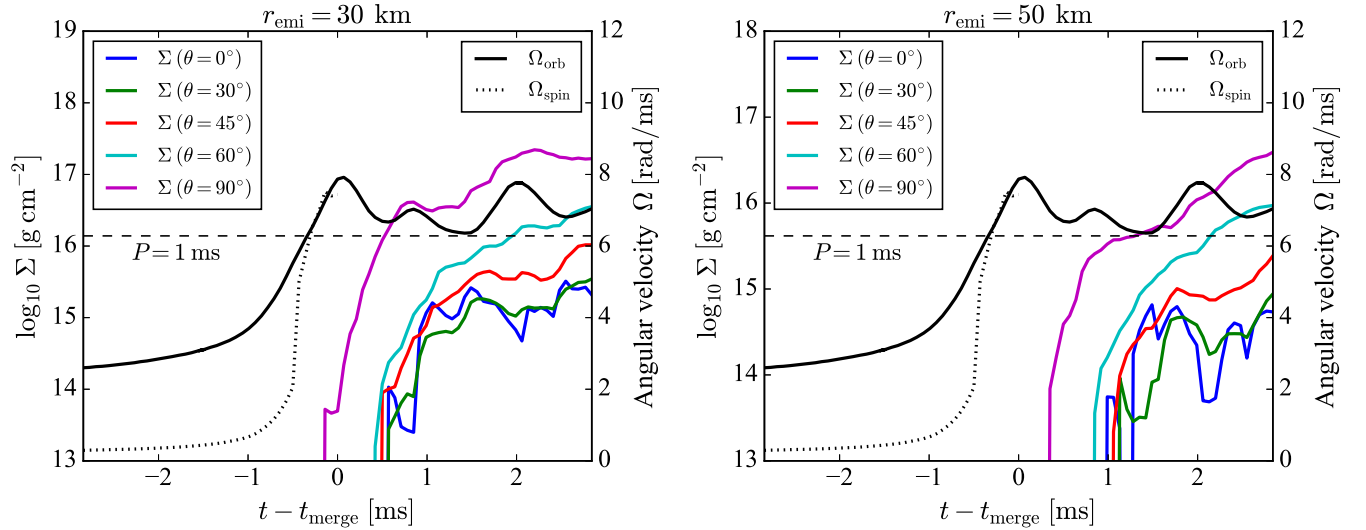


**Fig. 2.** Evolution of angular velocities of orbital motion ( $\Omega_{\text{orb}}$ ) and spin of each neutron star ( $\Omega_{\text{spin}}$ ) are shown by solid and dotted black curves, respectively (see the right hand ordinate for labels). The horizontal dashed line indicates  $\Omega$  corresponding to a rotation period of 1 ms. Color curves show rest-mass column density  $\Sigma$  in regions of  $r > r_{\text{emi}}$  towards the direction polar angle  $\theta$  from the  $z$  axis, for several values of  $\theta$ . The left and right panels are for  $r_{\text{emi}} = 30$  and 50 km, respectively, and a median about the azimuth angle  $\phi$  is taken for  $\Sigma$ .

ity  $\Omega_{\text{orb}}$  is simply calculated by setting the rotation center at the center of the simulation box and integration over the whole simulation box. The spin of each neutron star  $\Omega_{\text{spin}}$  is calculated by setting the rotation center at the density peak of one of the two neutron stars. For the integration region of  $\Omega_{\text{spin}}$ , we separate the simulation box into two by a plane including the simulation box center and perpendicular to the line connecting the two centers of the neutron stars. Then the integration of  $\Omega_{\text{spin}}$  is performed only over the half side including the neutron star considered. As expected,  $\Omega_{\text{spin}}$  of the two neutron stars are almost the same, and it becomes the same as  $\Omega_{\text{orb}}$  after the merger.

Though the calculation of  $\Omega_{\text{orb}}$  is completely Newtonian, we compare this with the angular frequency of the dominant quadrupole mode of gravitational wave radiation ( $\Omega_{\text{gw}}$ ) calculated from the simulation by a relativistic method using the Weyl scalar (Yamamoto et al. 2008). We then confirmed that the expected relation,  $\Omega_{\text{orb}} = \Omega_{\text{gw}}/2$ , holds within a 10% accuracy.

It can be seen in figure 2 that  $\Omega_{\text{orb}}$  gradually increases to the merger, but  $\Omega_{\text{spin}}$  suddenly rises up at  $\sim 0.5$  ms before the merger. Our simulation does not include viscosity, and hence a tidal lock by viscosity does not occur. A tidal lock is not expected to occur even if viscosity is taken into account (Bildsten & Cutler 1992). After the sharp rise,  $\Omega_{\text{spin}}$  is almost the same as  $\Omega_{\text{orb}}$ , and energy for FRBs can be extracted by the spin of magnetic fields of the merging star with a rotation period of about 1 ms. A coherent dipole magnetic field may be that of neutron stars before the merger, or may be formed during the merger process. The energy loss rate of the dipole emission formula is proportional to  $\Omega_{\text{spin}}^4$ , and hence the chance of producing an FRB rapidly increases at  $\sim 0.5$  ms before the merger.

### 3.2 Ejecta formation

Next we consider ejecta distribution. Figure 2 shows the time evolution of the rest-mass column density,

$$\Sigma(\theta, \phi; r_{\text{emi}}) = \int_{r_{\text{emi}}}^{\infty} \rho(\mathbf{r}) dr, \quad (3)$$

which is integrated over the radial direction from the simulation center excluding the inner region of  $r < r_{\text{emi}}$ , where  $r, \theta, \phi$  are spherical coordinates. As mentioned in section 2, low density grids with  $\rho < \rho_{\text{th}}$  are excluded from this calculation. We show the cases of  $r_{\text{emi}} = 30$  and 50 km, for several values of polar angle  $\theta$  from the  $z$  direction. The light cylinder radius becomes  $\sim 50$  km for a rotation period of 1 ms, and hence it is reasonable to expect that FRB radiation occurs at 30–50 km from the center. The column density also depends on the azimuth angle  $\phi$ , and here we take the median of  $\Sigma(\phi_i)$  to show a typical column density, where  $\phi_i$  is the 360 grids in  $\phi = 0-2\pi$  to calculate  $\Sigma$ . (We avoid a simple mean because it is biased when a high den-

sity ejecta exist into one direction, though its covering fraction on the sky is small.)

This figure shows that  $\Sigma$  significantly increases 0–1 ms after the merger. Ejecta to the equatorial directions ( $\theta \sim 90^\circ$ ) appear earlier, because dynamical mass ejection is driven first by tidal force, and then shock heated components are ejected to the polar direction from the HMNS (Sekiguchi et al. 2015). Since the minimum density resolved in the simulation is  $10^8 \text{ g cm}^{-3}$ , column density of  $\Sigma \lesssim 10^{14} \text{ g cm}^{-2}$  cannot be resolved on the scale of 30–50 km. Once  $\Sigma$  becomes larger than this, there is no chance for an FRB emission to escape, because the optical depth of electron scattering is many orders of magnitudes larger than unity. The rapid increase of  $\Sigma$  by many orders of magnitude occurs at about 1 ms after the merger to most of directions, implying that the environment before this is similar to that of isolated neutron stars.

Figure 3 shows time snapshots of radial profiles of rest-mass density and velocity. Here, again the median is plotted about the azimuth angle. Except for the equatorial ( $\theta = 90^\circ$ ) direction, the density sharply drops from  $10^{14}$  to  $\sim 10^9 \text{ g cm}^{-3}$  at the surface of newly born HMNS. An extended tail of the density profile at  $\rho \sim 10^8 \text{ g cm}^{-3}$  is seen, but it may be an artifact because this low density is close to the simulation resolution. Well-resolved ejecta with  $\rho \gg 10^8 \text{ g cm}^{-3}$  and positive radial velocity are seen only into the equatorial direction at the time of merger, and those into other directions appear a few ms after the merger. The ejecta velocity is at most 0.1–0.2 $c$ , and it takes about 1 ms for such an ejecta to expand into the outer regions of  $r > r_{\text{emi}} \sim 30-50$  km.

These results imply that a significant ejecta formation and expansion to the scale of 30–50 km occurs about 1 ms after the merging neutron stars start to rapidly spin. Therefore there is a short time window of  $t - t_{\text{merge}} \sim -0.5$  to 0.5 ms in which the ejecta is not yet formed but the magneto-rotational energy production rate is sufficiently high to produce an FRB emission. This also gives a possible explanation for the observed  $\sim 1$  ms duration of non-repeating FRBs.

## 4 Repeating FRBs from the Remnant Neutron Star after a BNS Merger

### 4.1 Formation of the Remnant Neutron Star and Its Environment

Hereafter we consider the case that a BNS merger leaves a merged neutron star that is indefinitely stable without rotation or rotationally supported for a time scale longer than the repeating FRB lifetime. Its initial spin period is  $P_1 = 2\pi/\Omega_i \sim 1$  ms, mass  $\sim 2.6M_\odot$ , and radius  $R \sim 15$  km. The rotational energy of the star is

$$E_{\text{rot}} = \frac{1}{2} I \Omega_i^2 \approx 9.2 \times 10^{52} \text{ erg}, \quad (4)$$

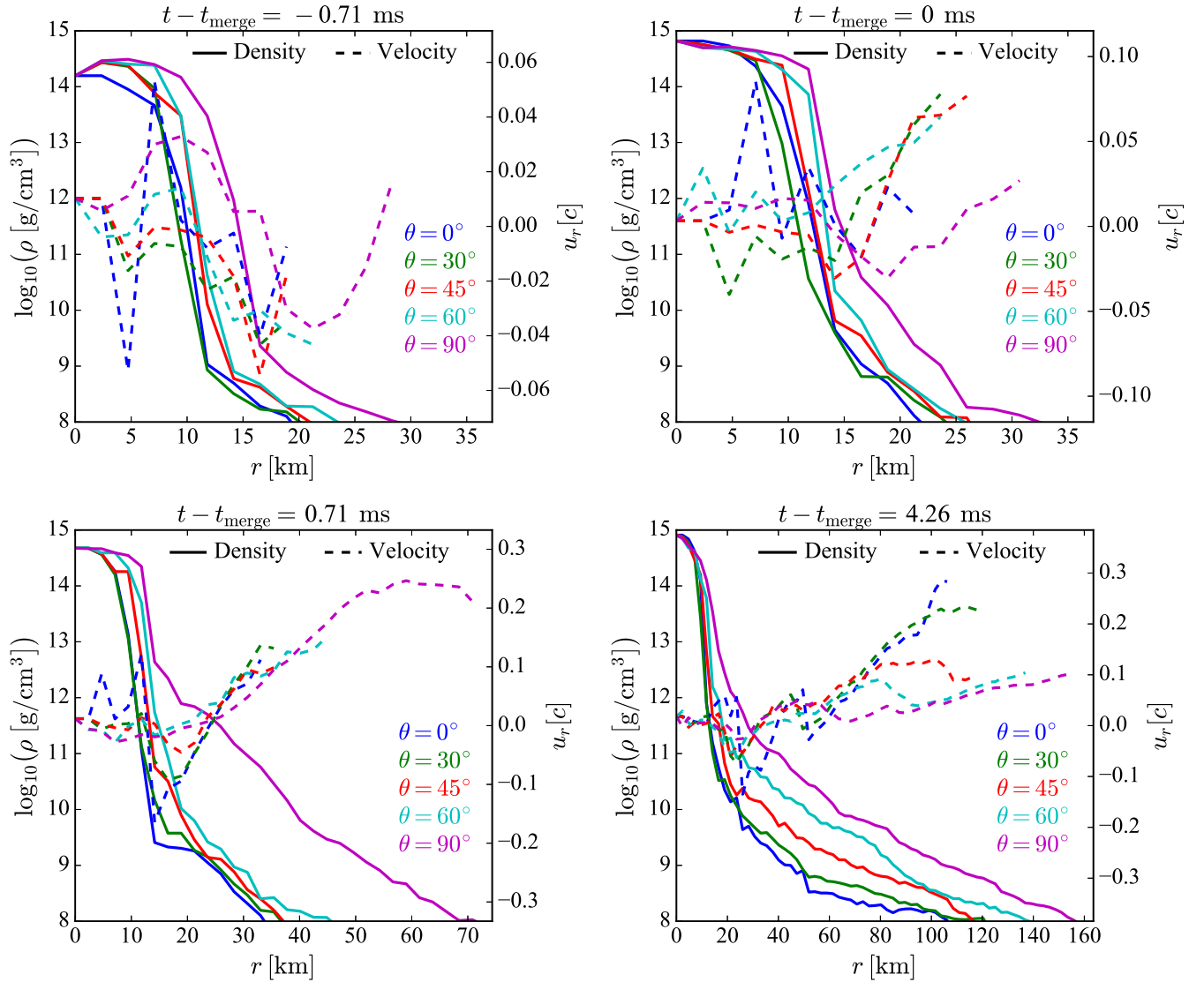


**Fig. 3.** Time snapshots (corresponding to figure 1) of radial profiles of rest-mass density (solid colored lines) and radial fluid velocity (dashed colored lines), for several values of polar angle  $\theta$  from the  $z$  axis. These quantities are the median about the azimuthal angle  $\phi$ . The radius is measured from the merger center.

where  $I$  is the momentum of inertia of the star. The spin-down timescale by magnetic breaking is given as

$$t_{\text{sd}} = \frac{3c^3 I P_i^2}{4\pi^2 B_*^2 R^6} \sim 2.7 B_{12.5}^{-2} \text{ yrs}, \quad (5)$$

where  $B_{12.5} = B_*/(10^{12.5} \text{ G})$  is the strength at the star surface. We adopt  $10^{12.5} \text{ G}$  as a reference value that is typical for isolated pulsars, but the magnetic field strength may be enhanced by the merger process to  $B \gtrsim 10^{13} \text{ G}$  as suggested by numerical simulations (e.g., Kiuchi et al. 2014), and in such a case  $t_{\text{sd}}$  could be smaller.

Consider ejecta mass  $M_{\text{ej}} = 10^{-3} M_\odot$  and velocity  $\beta_{\text{ej},0} = v_{\text{ej},0}/c = 0.1$ , which are within the typical ranges for a BNS merger. The dynamical ejecta mass decreases with stiffer EOS (Hotokezaka et al. 2013), and the ejecta mass may be enhanced

by disk wind (Shibata et al. 2017). The ejecta kinetic energy would be changed when the rotation energy of the newly born massive neutron star is injected into the merger ejecta in the form of pulsar wind, within a time scale of  $t_{\text{sd}}$ . Assuming that an energy of  $E_{\text{rot}}$  is injected as relativistic particles or Poynting flux at a radius  $r_{\text{inj}} = v_{\text{ej},0} t_{\text{sd}}$ , we can estimate the accelerated velocity and internal energy of ejecta (pulsar wind nebula) to be  $\beta_{\text{PWN}} = 0.98$  and  $U_{\text{inj}} = 1.6 \times 10^{52} \text{ erg}$ , respectively, from energy and momentum conservation. We assume that ejecta is freely expanding except for the velocity change at  $r = r_{\text{inj}}$ . The expanding ejecta would be decelerated by interstellar medium (ISM) when a comparable ISM has been swept up, but this effect can be ignored if we consider evolution before the deceleration time  $t_{\text{dec}} \sim 7.0 M_{\text{ej},-3}^{1/3} n_{\text{ISM},-3}^{-1/3} \beta_{\text{PWN}}^{-1} \text{ yr}$ , where  $n_{\text{ISM}} = 10^{-3} n_{\text{ISM},-3} \text{ cm}^{-3}$  is the ISM density. Note that

$t_{\text{dec}}$  becomes larger if the ejecta mass is larger than the assumed  $10^{-3}M_{\odot}$ . In this work we do not consider the interaction with ISM for simplicity.

The energy injection by pulsar wind would also generate magnetic fields in the ejecta. We assume a fraction  $\epsilon_B$  of the internal energy is carried by the magnetic fields at the time of injection ( $r = r_{\text{inj}}$ ), as  $B_{\text{ej},\text{inj}}^2/(8\pi) \approx \epsilon_B u_{\text{inj}}$ , where  $u_{\text{inj}}$  is the internal energy density. If the magnetic flux is conserved, the ejecta magnetic field strength evolves as  $B_{\text{ej}} = B_{\text{ej},\text{inj}}(r/r_{\text{inj}})^{-2}$  with the ejecta radius  $r$ , which then reduces to

$$B_{\text{ej}} = 1.7 \times 10^{-2} \epsilon_{B,-2}^{1/2} B_{12.5}^{-1} \beta_{\text{PWN}}^{-2} t_{\text{yr}}^{-2} \text{ G}, \quad (6)$$

where  $t_{\text{age}} = t_{\text{yr}}$  yr is the time elapsed from the merger, and we use  $\epsilon_{B,-2} = \epsilon_B/10^{-2}$  that is inferred from the magnetization parameter of the Crab nebula (Kennel & Coroniti 1984). Here we assumed the shell thickness  $\Delta r \sim r$  to calculate  $u_{\text{inj}}$ . The dependence on  $B_*$  appears by  $t_{\text{sd}}$  (smaller  $r_{\text{inj}}$  for stronger  $B_*$ ). Note that we made an approximation of  $t_{\text{age}} \sim r/v_{\text{PWN}}$ , which is exactly valid only when  $t_{\text{age}} \gg t_{\text{sd}}$ . This does not affect the conclusions in this section from order-of-magnitude estimates. This magnetic field strength will be used in the next section to discuss the energetics of synchrotron radiation and rotation measure.

## 4.2 Comparison with FRB 121102 observations

First we estimate the time scale for the ejecta to become transparent to the free-free absorption of radio signals. Before energy injection by pulsar wind, the opacity becomes less than unity at a time

$$t_{\text{tr}} \sim 1.6 (Z/50) f_{\text{ion}}^{1/5} \nu_9^{-2/5} T_{e,4}^{-3/10} \times M_{\text{ej},-3}^{2/5} (\beta_{\text{ej},0}/0.1)^{-6/5} \text{ yr} \quad (7)$$

after the merger, where  $\nu_9 \equiv \nu/(\text{GHz})$  is the frequency of the radio signal,  $f_{\text{ion}}$  is the ionization fraction,  $Z$  the mean atomic number, and  $T_{e,4} = T_e/(10^4 \text{ K})$  the temperature of ejecta. After the energy injection by pulsar wind, electrons in the ejecta may have relativistic energies (the Lorentz factor  $\gamma_e \sim 1$  or much larger if energy conversion from ions to electrons is efficient). Since the free-free opacity of relativistic electrons is reduced compared with non-relativistic ones (Kumar et al. 2017), the environment would be transparent after the energy injection.

Therefore the environment around a BNS merger would become transparent for a repeating FRB with a time scale of order years, though the uncertainty is more than one order of magnitude. After the appearance of a repeating FRB for an observer, the activity would decrease with time if the neutron star is already in the spin-down phase. Then the highest activity of a repeating FRB would last on a time scale similar to that of the appearance, i.e., of order years.

The source size of the persistent radio emission from FRB

121102 is limited to  $\lesssim 0.7 \text{ pc}$  (Marcote et al. 2017), and this gives an upper limit on the age  $t_{\text{age}}$  of this source. Assuming that the ejecta is expanding with  $\beta_{\text{PWN}}$  from the beginning (i.e.,  $t_{\text{sd}} \ll t_{\text{age}}$ ), we find

$$t_{\text{age}} < 2.3 \left( \frac{\beta_{\text{PWN}}}{0.98} \right)^{-1} \text{ yr}, \quad (8)$$

which is comparable with the minimum age  $\sim 5 \text{ yr}$  of FRB 121102. Therefore expanding size evolution of the persistent radio source may be observed in the near future, though a realistic morphology must be considered for a more quantitative prediction. The source size may be smaller if  $\beta_{\text{PWN}}$  is smaller by a larger ejecta mass, or  $t_{\text{sd}}$  is comparable to the age. Another possibility to make the size smaller is confinement by dense ISM.

The observed luminosity of the persistent radio emission from FRB 121102 ( $1.9 \times 10^{39} \text{ erg s}^{-1}$  at 10 GHz, Chatterjee et al. 2017) can be used to estimate the minimum electron energy emitting synchrotron radiation. Following the formulation of Kashiyama & Murase (2017) and the magnetic field strength estimated above, we find the minimum electron energy as  $\sim 1.2 \times 10^{49} t_{\text{yr}}^3 \epsilon_{B,-2}^{-1/2} \beta_{\text{PWN}}^{3/2} \text{ erg}$ . This is sufficiently smaller than the maximum energy available by the rotation of the merged neutron star,  $E_{\text{rot}} \sim 10^{53} \text{ erg}$ , if the age is less than  $\sim 10 \text{ yrs}$ .

Next we consider dispersion measure (DM) around the remnant neutron star. DM of ejecta matter (after energy injection by the pulsar wind) using the standard formula becomes

$$\text{DM}_{\text{ej}} \approx 5.2 \times 10^{-2} M_{\text{ej},-3} f_{\text{ion}} \beta_{\text{PWN}}^{-2} t_{\text{yr}}^{-2} \text{ pc cm}^{-3}. \quad (9)$$

The DM contribution from the host galaxy of FRB 121102 is estimated as  $\text{DM}_{\text{host}} < 55\text{--}225 \text{ pc cm}^{-3}$  (Tendulkar et al. 2017; Kokubo et al. 2017), and the DM changing rate is constrained as  $< 2 \text{ pc cm}^{-3} \text{ yr}^{-1}$  (Piro 2016). These constraints can be easily met in our model if the age is larger than  $\sim 1 \text{ yr}$ .

Though rotation measure (RM) is not yet measured for the repeating FRB 121102, it has been observed for some FRBs. Masui et al. (2015) found a relatively large RM contribution from the host galaxy ( $\gtrsim 160 \text{ rad m}^{-2}$ ) of FRB 110523, which favors a dense and magnetized environment like star forming regions or supernova remnants. On the other hand, small or negligible RMs from the host galaxy and IGM were observed for the exceptionally bright FRB 150807 ( $\lesssim 2 \text{ rad m}^{-2}$ , Ravi et al. 2016) and FRB 150215 ( $< 25 \text{ rad m}^{-2}$ , Petroff et al. 2017), which favor a cleaner environment.

We can calculate RM of the ejecta matter in our model assuming that the magnetic field is ordered along the line of sight to an observer, which becomes

$$\text{RM}_{\text{ej}} \sim 7.2 \times 10^2 \epsilon_{B,-2}^{1/2} B_{12.5}^{-1} \times M_{\text{ej},-3} f_{\text{ion}} \beta_{\text{PWN}}^{-4} t_{\text{yr}}^{-4} \text{ rad m}^{-2}. \quad (10)$$

This can be consistent even with the low RMs of FRB 150807

and FRB 150215 if we take  $t_{\text{yr}} \sim 10$ , though dependence on model parameters is large. Therefore it is possible that these apparently non-repeating FRBs are also remnant neutron stars after a BNS merger, and repeating has not yet been detected because of a search sensitivity and/or limited monitoring time. Of course, another possibility is that these FRBs were produced at the time of a BNS merger, for which we expect even smaller RM.

It should be noted that here we used the standard classical formulae for DM and RM calculations. However, electrons may have relativistic energy after the energy injection from pulsar wind. The relativistic effect reduces both DM and RM (Shcherbakov 2008), and hence this does not affect the consistency between our model and observations.

### 4.3 Comparison with the Supernova Scenarios

Supernovae, especially the class of SLSNe, have been proposed as the progenitor of a young and rapidly rotating neutron star to produce repeating FRBs (Kashiyama & Murase 2017; Metzger et al. 2017; Beloborodov 2017; Dai et al. 2017). Here we compare the SN scenario with our BNS merger scenario. Besides the event rate difference between SLSNe and BNS mergers mentioned in section 1, a large difference is the ejecta mass of SLSNe that is much larger than that of BNS mergers. Here we discuss using typical parameter values of  $M_{\text{ej},1} \equiv M_{\text{ej}}/(10M_{\odot})$  and  $v_{\text{ej},9} \equiv v_{\text{ej}}/(10^9 \text{ cm/s})$  (i.e., an explosion energy of  $10^{52}$  erg) for a SLSN (Metzger et al. 2017). The difference would be smaller in the case of ultra-stripped SLSNe ( $M_{\text{ej}} \sim 0.1M_{\odot}$ , Kashiyama & Murase 2017), but the event rate of such supernovae would be even smaller than that of SLSNe.

Because of the larger mass ejecta and slower speed, it would take a longer time for the environment to become transparent for radio signals. The previous studies about the SLSN scenario then considered a time scale of 10–100 yrs as the age of FRB 121102. Assuming that the spin-down time of a newly born neutron star is less than  $\sim 10$  yrs, the rotation energy is decreasing with time and hence we expect that the BNS scenario has a larger available rotation energy to produce FRBs than the SLSN scenario. Therefore even if the event rate of the two populations is the same, we expect brighter and more active FRBs from neutron stars produced by a BNS merger, and hence a higher chance of detection.

DM, source size and energetics of persistent radio emission in the SLSN scenario have been discussed in the previous studies, and they are consistent with observational constraints of FRB 121102. Compared with the BNS merger scenario, DM is larger and hence DM variability would be stronger, while the persistent radio source size is smaller and hence the size upper limit is more easily met. RM in the SLSN scenario has not been discussed in the previous studies, and from our formulations we

find

$$\text{RM}_{\text{ej}} \sim 1.7 \times 10^{11} \epsilon_{\text{B},-2}^{1/2} B_{14}^{-1} \times M_{\text{ej},1} f_{\text{ion}} v_{\text{ej},9}^{-4} t_{\text{yr}}^{-4} \text{ rad m}^{-2}. \quad (11)$$

Here we assumed that the ejecta has an internal energy of  $\sim 10^{52}$  erg at the time of the energy injection from pulsar wind, but the velocity is not accelerated because the original supernova kinetic energy is comparable with the energy injected by the pulsar wind. This RM is much larger than the maximum RM found for FRB 110523, even if we assume an age of 100 yrs and a strong stellar magnetic field of  $B_* = 10^{14} B_{14}$  G. This implies that all FRBs cannot be a young neutron star produced by a SLSN, unless the net magnetization is largely cancelled by small scale fluctuations of magnetic field directions.

## 5 Rate Evolution of Repeating and Non-repeating FRBs

### 5.1 Cosmic BNS merger rate evolution

In order to discuss about the FRB detection rate as a function of a search sensitivity, we first determine the cosmic BNS merger rate as a function of redshift. The comoving volumetric BNS merger rate at a redshift  $z$  [corresponding to a cosmic time  $t(z)$ ] is a convolution of the comoving star formation rate density  $\Psi_{\text{SFR}}$  and the delay time distribution (DTD) of BNS mergers from star formation:

$$\mathcal{R}_{\text{BNS}}(z) = \int_0^{t(z)} \Psi_{\text{SFR}}(t - \tau) f_{\text{D}}(\tau) d\tau, \quad (12)$$

where  $\tau$  is the delay time (the time elapsed from the formation of a stellar binary to the BNS merger), and  $f_{\text{D}}(\tau)$  is DTD normalized per unit mass of star formation.

We use a functional form of cosmic star formation history,

$$\Psi_{\text{SFR}}(z) = 0.015 \frac{(1+z)^{2.7}}{1 + [(1+z)/2.9]^{5.6}} M_{\odot} \text{ yr}^{-1} \text{ Mpc}^{-3} \quad (13)$$

in  $0 < z < 8$  derived by Madau & Dickinson (2014). DTD of compact object mergers generally becomes  $f_{\text{D}} \propto \tau^{-\alpha}$  with  $\alpha \sim 1$ , when it is controlled by gravitational wave radiation as in the cases of BNS or binary white dwarfs (e.g., Totani et al. 2008). Here we set  $f_{\text{D}} \propto \tau^{-1}$  at  $\tau \geq \tau_{\text{min}}$  and zero otherwise, with  $\tau_{\text{min}} = 10$  Myr, which is roughly consistent with that calculated by Belczynski et al. (2006) using a binary population synthesis model. The BNS merger rate is normalized as  $\mathcal{R}_{\text{BNS}}(0) = 1 \times 10^4 \text{ Gpc}^{-3} \text{ yr}^{-1}$ , which is the ‘‘plausible optimistic’’ rate estimate for local BNS mergers by Abadie et al. (2010). It should be noted that the following results on the ratio of repeating to non-repeating FRB rates is not affected by this normalization. The calculated  $\Psi_{\text{SFR}}(z)$  and  $\mathcal{R}_{\text{BNS}}(z)$  are shown in figure 4.

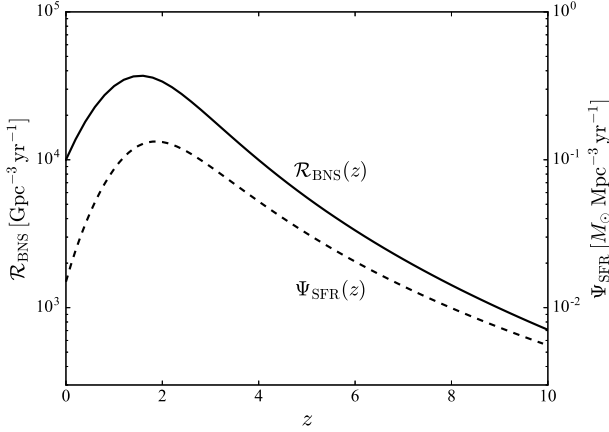


**Fig. 4.** Cosmic star formation rate  $\Psi_{\text{SFR}}$  (dashed line, right-hand-side ordinate) and cosmic BNS merger rate  $\mathcal{R}_{\text{BNS}}$  (solid line, left-hand-side ordinate) per unit comoving volume in our model are shown as a function of redshift  $z$ .

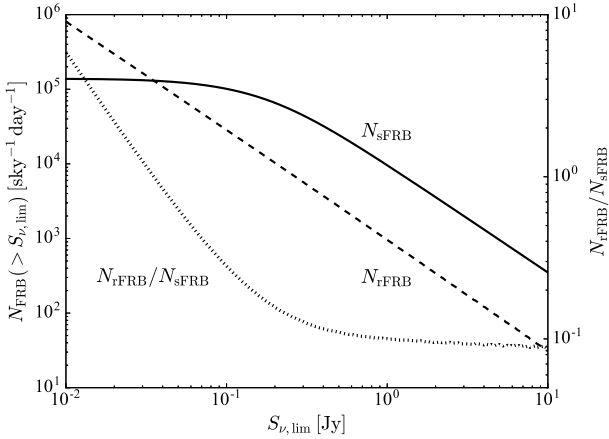


**Fig. 5.** Occurrence rate of FRBs that are brighter than a search flux sensitivity limit, for non-repeating (single) FRBs ( $N_{\text{sFRB}}$ ) and repeating FRBs ( $N_{\text{rFRB}}$ ). The repeating FRB rate is normalized as 10% of non-repeating FRBs at  $S_{\nu,\text{lim}} = 1$  Jy (i.e.,  $f_r N_r = 400$ ). The ratio  $N_{\text{rFRB}}/N_{\text{sFRB}}$  is also plotted (see ordinate on the right hand side).

## 5.2 Repeating versus Non-repeating FRB Detection Rates

The FRB luminosity function is hardly known, and for simplicity we adopt the standard candle approximation both for the non-repeating and repeating populations. There is a large variation in radio spectral index of FRBs (e.g., Spitler et al. 2014), and here we simply assume  $L_\nu \propto \nu^0$ , and hence  $S_\nu \propto (1+z)D_L(z)^{-2}$ , where  $L_\nu$  is the absolute FRB luminosity per unit frequency,  $S_\nu$  the observed flux density, and  $D_L$  the luminosity distance. The absolute luminosity is fixed so that  $S_\nu = 1.0$  Jy at  $z = 1$  for non-repeating FRBs based on fluxes and DMs observed by Parkes, while  $S_\nu = 0.1$  Jy at  $z = 0.19$  for repeating FRBs based on the case of FRB 121102.

Then the all-sky rates for single (i.e., non-repeating) FRBs ( $N_{\text{sFRB}}$ ) and repeating FRBs ( $N_{\text{rFRB}}$ ) that are brighter than a

limiting flux density  $S_{\nu,\text{lim}}$  are calculated using  $\mathcal{R}_{\text{BNS}}(z)$  as:

$$N_{\text{sFRB}}(> S_{\nu,\text{lim}}) = \int_0^{z_s} dz \frac{dV}{dz} \frac{\mathcal{R}_{\text{BNS}}}{1+z}, \quad (14)$$

$$N_{\text{rFRB}}(> S_{\nu,\text{lim}}) = \int_0^{z_r} dz \frac{dV}{dz} \frac{\mathcal{R}_{\text{BNS}}}{1+z} f_r N_r, \quad (15)$$

where  $dV/dz$  is the comoving volume element per unit redshift,  $(1+z)^{-1}$  is the cosmological time dilation factor, and  $z_s(S_{\nu,\text{lim}})$  and  $z_r(S_{\nu,\text{lim}})$  are the redshifts corresponding to single and repeating FRBs with a flux  $S_{\nu,\text{lim}}$ , respectively. In the case of repeating FRBs, the formation probability of a repeating FRB source after a BNS merger ( $f_r$ ) and the number of repeating bursts during its lifetime ( $N_r$ ) are multiplied. Here we assumed that all BNS mergers produce a non-repeating FRB at the time of merger, and assumed the same beaming factor for the two populations. These assumptions also affect the ratio  $N_{\text{sFRB}}/N_{\text{rFRB}}$ , and uncertainties about these can be included in the parameter  $f_r$ .

No repeating FRBs have been detected by Parkes, and it implies

$$\frac{N_{\text{rFRB}}}{N_{\text{sFRB}} \big|_{S_{\nu,\text{lim}}=1 \text{ Jy}}} \lesssim 0.1, \quad (16)$$

which translates into an upper limit on the product  $f_r N_r \lesssim 400$ . The parameter  $N_r$  can be written as  $N_r = \tau_t k \zeta$ , where  $\tau_t$  is the lifetime of a repeating FRB source,  $k$  the repeat rate during the active FRB phase, and  $\zeta$  the active duty cycle. Observationally inferred values are  $k \sim 3 \text{ day}^{-1}$  and  $\zeta \sim 0.3$  (Nicholl et al. 2017), and we get  $f_r \tau_t \lesssim 1.2 \text{ yr}$ . In order for the lifetime to be consistent with that discussed in section 4, a weak constraint of  $f_r \lesssim 0.1$  is obtained, though there is a large dependence on model parameters.

In figure 5, a log  $N$ -log  $S$  plot for sFRBs and rFRBs is shown. Both populations show the trend of  $N(> S_{\nu,\text{lim}}) \propto S_{\nu,\text{lim}}^{-1.5}$  in the bright flux limit, as expected when cosmological effects are negligible. The curve of non-repeating FRBs becomes flat at  $S_{\nu,\text{lim}} \lesssim 200 \text{ mJy}$  by the cosmological effects (cosmic volume and the BNS rate evolution), but such a behavior is not seen for repeating FRBs because their redshifts are lower and hence cosmological effects are small. The ratio  $N_{\text{rFRB}}/N_{\text{sFRB}}$  is also plotted in the figure 5. This rapidly increases with improving sensitivity at  $S_{\nu,\text{lim}} \lesssim 1 \text{ Jy}$ , because the cosmological effects work only on non-repeating FRBs. This gives a possible explanation for the fact that the only repeating FRB was discovered by Arecibo that has a better flux sensitivity than Parkes.

## 6 Discussion and Conclusions

In this paper, we investigated BNS mergers as a possible origin of both repeating and non-repeating FRBs.

Non-repeating and bright FRBs mostly detected by Parkes

may be produced at the time of a BNS merger, but the environment around the merger may be polluted by dynamical ejecta, which would prohibit radio signals to propagate. We therefore investigated the BNS merger environment using a general-relativistic hydrodynamical simulation. It was found that a significant mass ejection that can be resolved by the current simulation occurs about 1 ms after the merger, and hence there is a time window of about 1 ms in which the magneto-rotational energy production rate has become the maximum to produce an FRB emission and the environment is not yet polluted. This also gives a possible explanation for the observed short duration ( $\lesssim 1$  ms) of non-repeating FRBs.

A fraction of BNS mergers may leave a stable remnant neutron star, and such an object may produce faint and repeating FRBs like FRB 121102 detected by Arecibo, after the environment becomes clear for radio signals. We showed that the environment becomes clear on a time scale of order years, and after that FRB activities would become weaker on a similar time scale by the pulsar spin-down. The persistent radio emission of FRB 121102 can be explained by a pulsar wind nebula energized by the remnant neutron star. The expected radio source size is marginally consistent with the observational upper limit, implying that a source size evolution may be observed in the future. DM expected for the radio emitting nebula is smaller than the observational estimate of DM from the host galaxy of FRB 121102, and the nebula RM is not significantly larger than those measured in some FRBs. Compared with the supernova scenario for young neutron stars to produce repeater FRBs, the BNS merger scenario predicts a shorter time scale for the appearance after the merger (or supernova) and a shorter active lifetime as a repeating FRB source. The environment around the young neutron star is more transparent with smaller DM and RM, while the source size of persistent radio emission is larger. Especially, the expected large RM implies that the supernova scenario cannot be applied to all FRBs because some FRBs show small RM.

We then constructed an FRB rate evolution model including these two populations. Requiring that the discovery rate of a repeating FRB source is less than 10% of that for non-repeating FRBs at the search sensitivity of Parkes, the lifetime of repeating FRB sources  $\tau_{\text{rt}}$  is constrained as  $f_r \tau_{\text{rt}} \lesssim 1.2$  yr, where  $f_r$  is the fraction of BNS mergers leaving a remnant neutron star that is stable on a time scale longer than  $\tau_{\text{rt}}$ . Then we obtain  $f_r \lesssim 0.1$  from  $\tau_{\text{rt}} \sim 1\text{--}10$  yrs obtained in section 4, which is not a strong constraint because it is an order-of-magnitude estimate. Since non-repeating FRBs are brighter and hence more distant at a given sensitivity, the slope of FRB source counts ( $\log N\text{--}\log S$ ) is flatter than that of repeating FRBs. Therefore the relative ratio of repeating to non-repeating FRB source counts should rapidly increase with improving search flux sensitivity. This gives a possible explanation to the fact that the only repeating

FRB 121102 was discovered by the most sensitive search using Arecibo, and such a trend can be confirmed with more FRBs detected in the future. It should be noted that this trend is expected even if repeating FRBs originate from supernovae rather than BNS mergers.

In addition to some predictions already mentioned above, the following predictions can be made based on our hypothesis. Originating from BNS mergers, both repeating and non-repeating FRBs should be found both in star-forming and elliptical galaxies. FRB 121102 was found in a dwarf star forming galaxy with low metallicity, and this may favor the SLSN scenario. However, a strong conclusion cannot be derived from only one event; BNS mergers should also occur in such galaxies. It is plausible that FRBs showing negligible RM (FRBs 150807 and 150215) occurred in quiescent galaxies such as elliptical galaxies.

If non-repeating FRBs are produced at the time of BNS mergers, the BNS merger rate must be close to the high end of the possible range discussed in the literature, and gravitational wave from a BNS merger should be detected soon by LIGO/VIRGO/KAGRA. A non-repeating FRB can in principle be detected coincidentally with gravitational wave from a BNS merger, but a wide-field FRB search covering a considerable fraction of all sky will be the key. If the location of a BNS merger detected by gravitational wave is accurately determined by electromagnetic wave counterparts, there is a good chance of discovering repeating FRBs  $\sim 1\text{--}10$  years after the merger, though the probability of leaving a stable neutron star depends on EOS of nuclear matter. A repeating FRB may also be found 1-10 years after a non-repeating FRB or a short gamma-ray burst (GRB), but they are generally more distant than BNS mergers detected by gravitational waves and hence repeating FRBs may be too faint to detect.

Though the fraction of BNS mergers leaving a stable neutron star is currently highly uncertain, gravitational wave observations may constrain the nuclear matter EOS in the near future (Lattimer & Prakash 2007). Such constraints would be useful to examine the validity of our scenario for repeating FRBs. If a repeating FRB is detected after a BNS merger, it would be an unambiguous proof of a surviving remnant neutron star, which would give an independent constraint on EOS. Another possible signature of a surviving neutron star is a persistent radio emission from the pulsar wind nebula like FRB 121102, or that from interaction between ejecta and ISM (Horesh et al. 2016).

Finally we comment on some intriguing recent observational studies. Ofek (2017) reported 11 luminous radio sources in nearby ( $< 108$  Mpc) galaxies with offsets from the nucleus, whose luminosities are similar to the persistent source associated with FRB 121102. The number density of these is  $\sim 5 \times 10^{-5}$  Mpc $^{-3}$ . Using the typical lifetime of repeating FRBs (10 yrs) in our hypothesis, a birth rate of  $\sim 5 \times 10^3$  yr $^{-1}$  Gpc $^{-3}$

is inferred, which is interestingly similar to the non-repeating FRB rate and the high end of the possible BNS merger rate range. Furthermore, 2 of the 11 sources are in galaxies of old stellar population (passive and elliptical), which cannot be produced from young stellar populations.

Perley et al. (2017) reported a new radio source (Cygnus A-2) at a projected offset of 460 pc from the nucleus of Cygnus A ( $z = 0.056$ ), which was detected in 2015 but was not present until 1997. The origin of this source is not yet clear, and a repeating FRB was not discussed as a possible origin in Perley et al. (2017). However we noticed that the unusually bright radio luminosity as a supernova,  $\nu L_\nu \approx 6 \times 10^{39} \text{ erg s}^{-1}$ , is interestingly similar (within a factor of a few) to that of the persistent radio emission of FRB 121102, while Cygnus A-2 is about three times closer to us. The luminosity and the appearance time scale imply that Cygnus A-2 may also be a pulsar wind nebula produced by a BNS merger remnant, and a radio monitoring of this may lead to a discovery of another repeating FRB source.

## Acknowledgments

We thank Kazumi Kashiyama, Koutarou Kyutoku, Masaru Shibata, and Toshikazu Shigeyama for discussion and support to this work. SY was supported by the Research Fellowship of the Japan Society for the Promotion of Science (JSPS) (No. JP17J04010). SY was also supported by a grant from the Hayakawa Satio Fund awarded by the Astronomical Society of Japan. TT was supported by JSPS KAKENHI Grant Numbers JP15K05018 and JP17H06362. KK was supported by JSPS KAKENHI Grant Numbers JP16H02183, JP15K05077, and JP17H06361, and by a post-K computer project (Priority issue No. 9) of MEXT, Japan. Numerical computations were performed on K computer at AICS (project number hp160211 and hp170230), on Cray XC30 at cfca of National Astronomical Observatory of Japan, FX10 and Oakforest-PACS at Information Technology Center of the University of Tokyo, and on Cray XC40 at Yukawa Institute for Theoretical Physics, Kyoto University.

## References

- Abadie, J., et al. 2010, *Classical and Quantum Gravity*, 27, 173001
- Abbott, B. P., Abbott, R., Abbott, T. D., et al. 2016, *Astrophys. Lett.*, 832, L21
- Belczynski, K., Perna, R., Bulik, T., Kalogera, V., Ivanova, N., & Lamb, D. Q. 2006, *ApJ*, 648, 1110
- Beloborodov, A. M. 2017, *ApJ*, 843(2), L26
- Bildsten, L., & Cutler, C. 1992, *ApJ*, 400, 175
- Chatterjee, S. et al., et al. 2017, *Nature*, 541, 58
- Connor L., Sievers, J., & Pen, U.-L. 2016, *MNRAS*, 458, L19
- Cordes, J. M., & Wasserman, I. 2016, *MNRAS*, 457, 232
- Dai, Z. G., Wang, J. S., Wu, X. F., & Huang, Y. F. 2016, *ApJ*, 829, 27
- Dai, Z. G., Wang, J. S., & Yu, Y. W. 2017, *Astrophys. Lett.*, 838, L7
- Dominik, M., Belczynski, K., Fryer, C., et al. 2013, *ApJ*, 779, 72
- Falcke, H., & Rezzolla, L. 2014, *ApJ*, 562, A137
- Gao, H., Zhang, B., Wu, X.-F., & Dai, Z.-G. 2013, *Phys. Rev. D*, 88, 043010
- Geng, J. J. & Huang, Y. F. 2015, *ApJ*, 809, 24
- Glendenning, N. K., & Moszkowski, S. A. 1991, *Phys. Rev. Lett.*, 67, 2414
- Hansen, B. M. S., & Lyutikov, M. 2001, *MNRAS*, 322, 695
- Hotokezaka, K., Kyutoku, K., Tanaka, M., Kiuchi, K., Sekiguchi, Y., Shibata, M., & Wanajo, S. 2013, *Astrophys. Lett.*, 778, L16
- Horesh, A., Hotokezaka, K., Piran, T., Nakar, E., & Hancock, P. 2016, *Astrophys. Lett.*, 819, L22
- Kashiyama, K., Ioka, K., & Mészáros, P. 2013, *Astrophys. Lett.*, 776, L39
- Kashiyama, K., & Murase, K. 2017, *ApJ*, 839, L3
- Keane, E. F., et al. 2016, *Nature*, 530, 453
- Kennel, C. F., & Coroniti, F. V. 1984, *ApJ*, 283, 710
- Kiuchi, K., Kyutoku, K., Sekiguchi, Y., Shibata, M., & Wada, T. 2014, *Phys. Rev. D*, 90, 041502
- Kokubo, M., et al. 2017, *ApJ*, 844, 95
- Kulkarni, S. R., Ofek, E. O., Neill, J. D., Zheng, Z., & Juric, M. 2014, *ApJ*, 797, 70
- Kumar, P., Lu, W., & Bhattacharya, M. 2017, *MNRAS*, 468, 2726
- Lai, D. 2012, *ApJ*, 757, L3
- Lattimer, J. M., & Prakash, M. 2007, *Physics Reports*, 442, 109
- Lorimer, D. R., Bailes, M., McLaughlin, M. A., Narkevic, D. J., & Crawford, F. 2007, *Science*, 318, 777
- Lyubarsky, Y. 2014, *MNRAS*, 442, L9.
- Madau, P., & Dickinson, M. 2014, *Annual Review of Astronomy and Astrophysics*, 52, 415
- Marcote, B., et al. 2017, *Astrophys. Lett.*, 834, L8
- Masui, K., et al. 2015, *Nature*, 528, 523
- Metzger, B. D., Berger, E., & Margalit, B. 2017, *ApJ*, 841, 14
- Metzger, B. D., & Piro, A. L. 2014, *MNRAS*, 439, 3916
- Mingarelli, C. M. F., Levin, J., & Lazio, T. J. W. 2015, *Astrophys. Lett.*, 814, L20
- Nicholl, M., Williams, P. K. G., Berger, E., Villar, V. A., Alexander, K. D., Eftekhari, T., & Metzger, B. D. 2017, *ApJ*, 843, 84
- Ofek, E. O. 2017, *ApJ*, 846, 44
- Perley, D. A., Perley, R. A., Dhawan, V., & Carilli, C. L. 2017, *ApJ*, 841, 117
- Petroff, E., et al. 2015, *MNRAS*, 454, 457
- Petroff, E., et al. 2016, *Astronomical Society of Australia*, 33, e045
- Petroff, E., et al. 2017, *MNRAS*, 469, 4465
- Piro, A. L. 2012, *ApJ*, 755, 80
- Piro, A. L. 2016, *Astrophys. Lett.*, 824, L32
- Piro, A. L., Giacomazzo, B., & Perna, R. 2017, *ApJ*, 844, L19
- Planck Collaboration, et al. 2016, *A&A*, 594, A13
- Popov, S.B., & Postnov, K.A. 2010, *arXiv:0710.2006*
- Quimby, R. M., Yuan, F., Akerlof, C., & Wheeler, J. C. 2013, *MNRAS*, 431, 912
- Ravi, V., et al. 2016, *Science*, 354, 1249
- Scholz, P., et al. 2016, *ApJ*, 833, 177
- Sekiguchi, Y., Kiuchi, K., Kyutoku, K., & Shibata, M. 2015, *Phys. Rev. D*, 91, 064059
- Shcherbakov, R. V. 2008, *ApJ*, 688, 695
- Shibata, M., Kiuchi, K., & Sekiguchi, Y. 2017, *Phys. Rev. D*, 95, 083005
- Spitler, L. G., et al. 2014, *ApJ*, 790, 101
- Spitler, L. G., et al. 2016, *Nature*, 531, 202
- Tendulkar, S. P., et al. 2017, *Astrophys. Lett.*, 834, L7
- Thornton, D., et al. 2013, *Science*, 341, 53
- Totani, T., Morokuma, T., Oda, T., Doi, M., and Yasuda, N. 2008, *PASJ*, 60, 1327

- Totani, T. 2013, *PASJ*, 65, L12
- Wang, J.-S., Yang, Y.-P., Wu, X.-F., Dai, Z.-G., & Wang, F.-Y. 2016, *Astrophys. Lett.*, 822, L7
- Williams, P. K. G., & Berger, E. 2016, *Astrophys. Lett.*, 821, L22
- Yamamoto, T., Shibata, M., & Taniguchi, K. 2008, *Phys. Rev. D*, 78, 064054
- Zhang, B. 2017, *Astrophys. Lett.*, 836, L32